Noise characteristics of an oscillator with a barium strontium titanate (BST) varactor

A. Victor, J. Nath, D. Ghosh, B. Boyette, J.-P. Maria, M.B. Steer, A.I. Kingon and G.T. Stauf

Abstract: The phase noise of an oscillator with a thin-film barium strontium titanate (BST) capacitive tuning element, or varactor, is characterised and benchmarked against the same oscillator with a silicon semiconductor junction varactor. Phase noise tracks closely with varactor Q within a specific voltage range as expected. Compared to the semiconductor varactor-based oscillator, the BST-based oscillator demonstrates reduced phase noise degradation near zero volts, but greater phase noise degradation when operated near breakdown.

1 Introduction

Tunable resonator design encompasses careful selection of device technology and circuit topology, and is paramount in realising voltage-controlled oscillators (VCOs) with low phase noise. This is particularly so with power oscillators, such as an MOPA (master oscillator power amplifier). MOPAs should permit cost-effective transmitters that minimise frequency translation circuits and do not require separate power amplifiers to realise high power sources. The necessary provision of wide tuning range and low phase noise dictates a tunable resonator that supports large peak RF power with low Q reduction and low modulation effects due to capacitance nonlinearity. A combination of active device selection and resonator tapping (with appropriate impedance transformation) mitigates the power handling requirements of the resonator. However, to achieve frequency tuning of an octave or greater while also supporting the development of large signal levels, significant coupling to the resonator is needed. This in turn requires a tuning element that supports a large RF voltage swing. The technique of stacking junction varactors using a combination of series back-to-back and parallel combinations of diodes is one approach to addressing this problem [1]. This leads to a rapidly increasing number of diodes with associated parasitic and manufacturability concerns. This technique does, however, successfully reduce diode-related distortion, reduces the potential for rectification and significantly increases the effective AC breakdown voltage. Consequently large RF swings can be supported.

In this paper we explore the potential of high-power VCOs employing barium strontium titanate (BST). BST is a ferroelectric material that has a large electric-field-dependent permittivity and simultaneously can have low dielectric loss. It has been used in the past to construct voltage-tunable capacitors used as tuning elements in tunable filters, small-signal VCOs, phase shifters and delay lines [2–6]. The capacitance tuning mechanism with a BST varactor derives from strong field dependence of the dielectric polarisability, whereas a semiconductor varactor utilises variable space charge depletion. The characteristics of oscillators using these two types of varactors can be expected to be different in terms of tuning voltage, tuning linearity, breakdown voltage and noise effects.

The BST varactor was fabricated using a metal organic chemical vapour deposition (MOCVD) process [7] achieving a nominal Q of 32 at zero volt bias measured at 10 MHz. The BST thin film was deposited on $Si/SiO_2/Pt$ and had platinum (Pt) top electrodes, which were patterned using the standard image reversal process [8].

Two 50-MHz VCOs were constructed that were identical except that one used a semiconductor junction varactor and the other a BST varactor. In addition, a lower frequency 11-MHz oscillator developing a high peak RF resonator voltage was investigated. Tuning range and phase noise characteristics of the VCOs are explored here. This work report is a feasibility study for microwave and millimetre-wave MOPAs.

2 Oscillator characteristics

The two most important performance parameters for varactor-based MOPAs are the tuning range and phase noise, both of which are affected by a large RF voltage swing across the varactor. The tuning range is determined largely by the ratio of the maximum to the minimum varactor capacitances and is reduced by parasitics. The tuning range for VCOs with BST and junction semiconductor varactors is further reduced by excess phase noise generated at large bias voltages where breakdown occurs. In addition semiconductor varactors experience forward conduction, which also results in high excess shot noise. Thus, the sum of the DC tuning voltage and the RF peak voltage must be limited. Another concern is the reduction of varactor Q as the varactor is tuned. Leeson [9] showed that for a feedback oscillator, phase noise and Q are related such that phase noise is inversely proportional to Q^2. Typically it is the reduction in Q that determines tuning voltage

IEE Proceedings online no. 20050068

doi:10.1049/ip-map:20050068

Paper first received 31st March and in revised form 21st June 2005

A. Victor is with the Department of Electrical and Computer Engineering, North Carolina State University, Raleigh, NC 27612, USA and also with Harris Corporation, NC 27560, USA

J. Nath and M.B. Steer are with the Department of Electrical and Computer Engineering, North Carolina State University, Raleigh, NC 27695, USA

D. Ghosh, B. Boyette, J.-P. Maria and A.I. Kingon are with the Department of Materials Science and Engineering, North Carolina State University, Raleigh, NC 27695, USA

G.T. Stauf is with ATMI, Danbury, CT 06810, USA

E-mail: mbs@ncsu.edu

constraints, as this tends to be the more important limit, but even so the excess phase noise that occurs at breakdown and forward conduction can limit tuning range.

3 Varactor tuning range

The purpose of this Section is to quantifiably relate the phase noise impairments described above to the tuning range of a varactor. Key parameters are the tank (the circuit without the varactor) Q, the minimum varactor Q; and the ratio of the minimum to the maximum varactor capacitances as limited by shot noise considerations.

3.1 Non-degraded tuning range

In this Section we develop an expression for the tuning range in terms of the capacitance of the tank circuit and the maximum and minimum varactor capacitance. We begin by defining the capacitance tuning range

$$\alpha \equiv C_{V0}/C_{VB} \tag{1}$$

as the ratio of the maximum capacitance C_{V0} (we take this as being at zero volts for both the junction and BST varactors) and the minimum capacitance C_{VB} at or near breakdown occurring at voltage V_B. It is particularly convenient to introduce α as it is a common data sheet specification for a varactor. The parameter α is fixed by varactor capacitance against voltage profile. For a semiconductor varactor α is in the range 2–14 for varactors with linearly-graded to hyper-abrupt junctions. However, semiconductor varactors with higher α have lower breakdown voltages and higher nonlinearity resulting in higher harmonic content. A low-loss BST varactor has an α in the range 1.4–3, but this is partly compensated by the ability to extend varactor tuning to zero volt bias as Q is not reduced by conduction as is the case with a junction varactor. So overall the choice of varactor and circuit conditions involves complex design trade-offs.

In this work, operation of the varactor is significantly below the frequency where ferroelectric losses contribute. Most significant loss is resistive loss of the metal interconnect, bond wire and package lead frame. Therefore, the unloaded Q of the varactor Q_V is introduced by modelling the varactor as a capacitor C_V with a frequency-independent series resistance R_S so that $Q_V = 1/(\omega C_V R_S)$. When the varactor is operated well below self-resonance, this model is known to be suitable for junction varactors and also fits the experimental data for BST varactors. The minimum Q, Q_{VM}, of BST and junction varactors occurs at maximum C_V near zero volts bias so that $Q_{VM} = 1/(\omega_{V\approx 0} C_{V0} R_S)$. Then the varactor Q at bias voltage V is

$$Q_V(V) = Q_{VM}\frac{C_{V0}}{C_V} \tag{2}$$

The next stage in the development is to incorporate the effects of the resonator, active device feedback network and parasitics. This first requires transformation of the composite network, Fig. 1*a*, into its parallel form, Fig. 1*b*, with

$$R_P = R_S\left(Q_V^2 + 1\right) \text{ and } C_{VP} = \frac{C_{VS}}{\left(1 + 1/Q_V^2\right)} \tag{3}$$

With $Q \geq Q_{VM}^2 \gg 1$ and replacing Q_V in (3) using (2) this becomes

$$C_{VP} \approx C_{VS} = C_V \text{ and } R_P = R_S Q_{VM}^2 (C_{V0}/C_V)^2 \tag{4}$$

The effect of the tank circuit connected to the varactor is incorporated by including its Q and resonant frequency. The parallel circuit of Fig. 1*b* without the varactor has

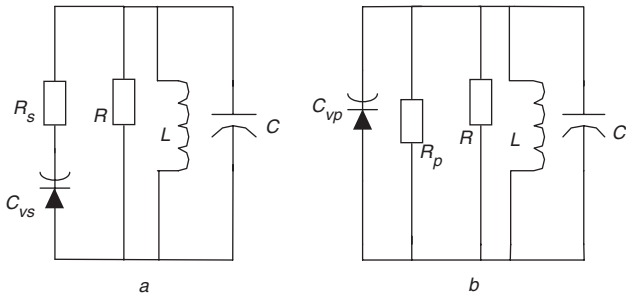

Fig. 1 *Varactor equivalent network representation*
a Simplified resonator and active device network with series varactor resistance R_s
b Transformed equivalent network with all elements in shunt

radian resonant frequency $\omega_0 = 1/\sqrt{LC}$ and Q

$$Q_0 = \omega_0 CR \tag{5}$$

We will utilise this Q in Section 3.3. With the varactor, the resonant frequency $\omega_{0V} = 1/\sqrt{L(C + C_{VP})}$ and this can be varied from ω_1 to ω_2 ($\omega_2 > \omega_1$) by tuning the varactor from zero volt bias to V_B so that

$$\omega_1 = 1/\sqrt{L(C + C_{V0})} \text{ and } \omega_2 = 1/\sqrt{L(C + C_{VB})} \tag{6}$$

This leads to the resonator tuning range χ defined as

$$\chi = (\omega_2 - \omega_1)/\omega_1 \tag{7}$$

which becomes

$$\chi = \left[\left(\frac{C}{C_{VB}} + \alpha\right) \Big/ \left(\frac{C}{C_{VB}} + 1\right)\right]^{1/2} - 1 \tag{8}$$

3.2 Effect of shot noise degradation

The tuning range derived above is reduced when excess shot noise is considered. In practice, a semiconductor varactor is not biased at zero volts because of the excess shot noise resulting when the RF swing drives the varactor into forward conduction. This effect does not occur with BST varactors, but the effective capacitance at zero volts is reduced by the RF voltage swing. The effect on the tuning capacitance achieved at low bias is captured by the parameter ε_1 so that the effective maximum capacitance is $\hat{C}_{V0} = C_{V0} - \varepsilon_1$. Both the BST and semiconductor varactors produce excess phase noise at high bias voltage. Thus, the effective minimum varactor capacitance is $\hat{C}_{VB} = C_{VB} + \varepsilon_2$. Then the minimum and maximum VCO tuning frequencies, respectively, are

$$\hat{\omega}_1 = 1 \Big/ \sqrt{L\left[C + \hat{C}_{V0}\right]} \text{ and } \hat{\omega}_2 = 1 \Big/ \sqrt{L\left[C + \hat{C}_{VB}\right]} \tag{9}$$

So the effective normalised tuning variable is now

$$\hat{\chi} = (\hat{\omega}_2 - \hat{\omega}_1)/\hat{\omega}_1 \tag{10}$$

or

$$\hat{\chi} = \left[\left(\frac{C}{\hat{C}_{VB}} + \frac{\hat{C}_{V0}}{\hat{C}_{VB}}\right) \Big/ \left(\frac{C}{\hat{C}_{VB}} + 1\right)\right]^{1/2} - 1 \tag{11}$$

The significance of this expression is that the fractional frequency tuning range is put in terms of the capacitances at the extremes of the tuning range plus the capacitance of the tank circuit. A more convenient form is obtained by defining the effective varactor tuning capacitance ratio as

$$\hat{\alpha} = \hat{C}_{V0}/\hat{C}_{VB} \tag{12}$$

and the effective normalised tuning variable becomes

$$\hat{\chi} = \left[\left(\frac{C}{\hat{C}_{VB}} + \hat{\alpha}\right) \Big/ \left(\frac{C}{\hat{C}_{VB}} + 1\right)\right]^{1/2} - 1 \qquad (13)$$

So $\hat{\chi}$ is less than χ reduced by the effect of the RF swing and shot nose considerations when the instantaneous voltage across the varactor approaches forward conduction (for a junction varactor) or breakdown (for either a junction and BST varactor).

3.3 Effect of Q degradation

Phase noise increases as the Q of the VCO resonant circuit decreases as the varactor is tuned from high bias voltages to near zero volts. To capture this effect in design, we introduce a Q degradation factor $\rho = Q_{0VM}/Q_0 (< 1)$, which is the ratio of the minimum circuit Q with the varactor to the Q of the tank circuit without the varactor. In design the desired tuning range is specified and whether this can be achieved is determined by the relationship between the maximum and minimum Qs of the varactor and the capacitance of the tank circuit. In this Section, we determine the Q degradation that must be tolerated in maintaining a desired tuning range. This is developed in terms of the minimum varactor Q and the Q of the tank circuit, and the degradation of Q leads to increased phase noise following Leesons' formula.

The tank circuit (without the varactor), the parallel circuit of Fig. 1*b*, has the following unloaded Q at resonant frequency ω_0:

$$Q_0 = \omega_0 CR \qquad (14)$$

With the varactor, the Q of the complete circuit is

$$Q_{0V} = \omega_{0V}(C + C_V)\left(\frac{1}{R} + \frac{1}{R_P}\right)^{-1} \qquad (15)$$

at the resonant frequency $\omega_{0V}(C_V) = 1/\sqrt{L(C + C_V)}$. Using (4), (15) becomes

$$Q_{0V} = \omega_{0V}(C + C_V)\left(\frac{RR_S Q_V^2}{R + R_S Q_V^2}\right) \qquad (16)$$

Now, we introduce the minimum varactor Q Q_{VM}. Q_{VM} occurs when the varactor capacitance is maximum, i.e. $C_V = \hat{C}_{VO}$

$$Q_{VM} = \frac{1}{\omega_{0V} R_S \hat{C}_{V0}} \qquad (17)$$

while the network Q without the varactor is given by (4) with $\omega_0 = \omega_{0V}$. The ratios of these Qs is a key design parameter and so we use

$$q = Q_0/Q_{VM} \qquad (18)$$

Varactors have limited Q and this is generally much less than that of the tank circuit (i.e. $Q_{VM} \ll Q_0$ and $q \gg 1$). After some algebra (see the Appendix) the Q degradation factor is obtained as

$$\rho = \frac{Q_{0VM}}{Q_0} = \left(\frac{q\hat{\alpha}(\hat{\chi}^2 + 2\hat{\chi})}{\hat{\alpha} - (\hat{\chi}^2 + 2\hat{\chi} + 1)} + 1\right)^{-1} + \frac{1}{q}\left[\frac{\hat{\alpha} - (\hat{\chi}^2 + 2\hat{\chi} + 1)}{\hat{\alpha} q(\hat{\chi}^2 + 2\hat{\chi})} + 1\right]^{-1} \qquad (19)$$

The importance of ρ is that phase noise is directly proportional to $1/\rho^2$ in the absence of excess noise sources (see Leeson [9]). So (19) relates the desired frequency tuning range $\hat{\chi}$ and the design parameter q (describing the tank Q and varactor Q) to phase noise degradation.

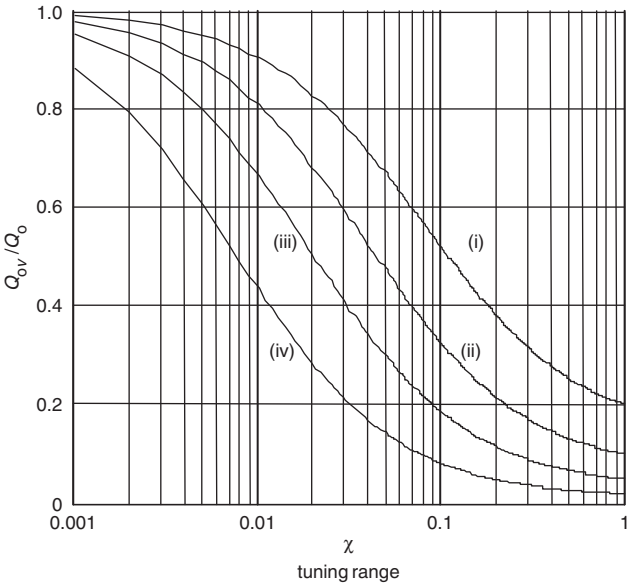

Fig. 2 *Calculated varactor tuning range against Q reduction for* $\hat{\alpha} = 2$ *and various q*
(i) $q = 5$; (ii) $q = 10$; (iii) $q = 20$; (iv) $q = 50$

Plots of ρ are shown in Fig. 2 with q as a running parameter while $\hat{\alpha} = 2$ is fixed (typical of the varactors considered in this paper). This plot can be used to manage the complicated trade-off between noise, varactor selection and tunability [10]. For low phase noise degradation it is desirable for ρ to be close to 1. We note that a varactor with a larger minimum varactor Q (smaller q) and allowable Q degradation (and so increase in the level of phase noise) will have an extended tuning range.

4 Results and observations

Two closely matched VCOs operating from 30–60 MHz were designed with the topology shown in Fig. 3. One of the VCOs used a semiconductor junction varactor and the other a BST-based varactor. The VCO topology uses a bipolar current-limited transformer feedback configuration with the varactor parallel tuned with the resonator. Utilising the design procedure outlined in the previous Section, the oscillators were designed to have the same tuning range and

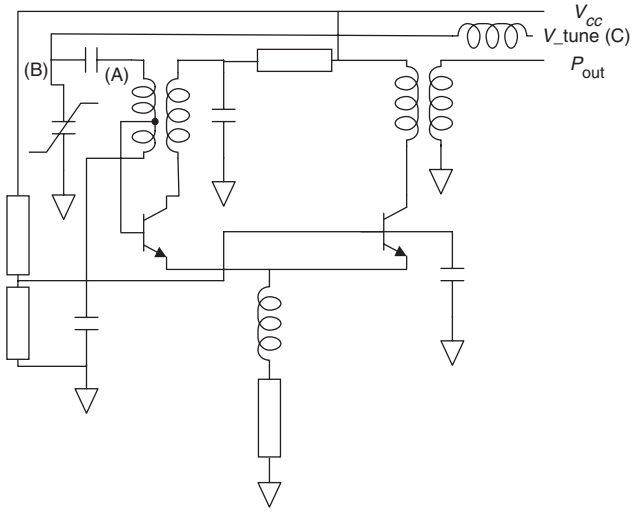

Fig. 3 *Circuit diagram of the VCO*

oscillator gain or K_o (Hz/V) value. A χ value of 0.2 is desired and using (8) a resonator capacitance is found in terms of the minimum varactor capacitance near breakdown C_{VB}. The $\hat{\chi}$ value is therefore more appropriate to use and results in two different values of shunt resonator capacitance for each varactor type as shown in Figs. 1 and 3. In this investigation the varactors had a nominal q of 13, from Fig. 2 a Q reduction factor of 0.18 is expected. To improve this reduction requires a decrease in q. The optimum resonator capacitance C with the BST and junction varactors is in the range 218–135 pF. The addition of a capacitance in series with the varactor effectively increases the breakdown voltage, decreases q and permits a smaller resonator capacitance. The combination of the shunt resonator capacitance, the series coupling capacitance with the varactor and the resonator inductance permits adjustment of the L/C ratio [11, 12] of the resonator, the tuning range, and the noise as influenced by the Q degradation factor ρ. These component values are determined for a specific oscillator gain. Thus, the performance of the VCOs can be equitably compared. The semiconductor and BST-based varactors had a capacitance tuning range α of nearly three. This degraded to an effective value of approximately two when the RF swing was taken into account. The semiconductor varactor was linearly graded with a capacitance index of nonlinearity approximating 0.35–0.39 over the full tuning range. This capacitance nonlinearity is only moderately nonlinear and so AM–PM conversion effects, which lead to increased phase noise, are expected to be small [13]. The breakdown voltage of the semiconductor varactor is 40 V. The BST varactor was previously reported in [8] and is of metal–insulator–metal (MIM) type and its breakdown voltage was 10 V. The capacitance and Q against tuning voltage of the BST-based varactor measured at 50 MHz is shown in Fig. 4. The varactor Q against frequency at a fixed reverse bias of 4 volts is calculated from the measured reactance and resistance against frequency (shown in Fig. 11). (Capacitance and Q were measured on a Hewlett Packard Model 4191A impedance analyser.)

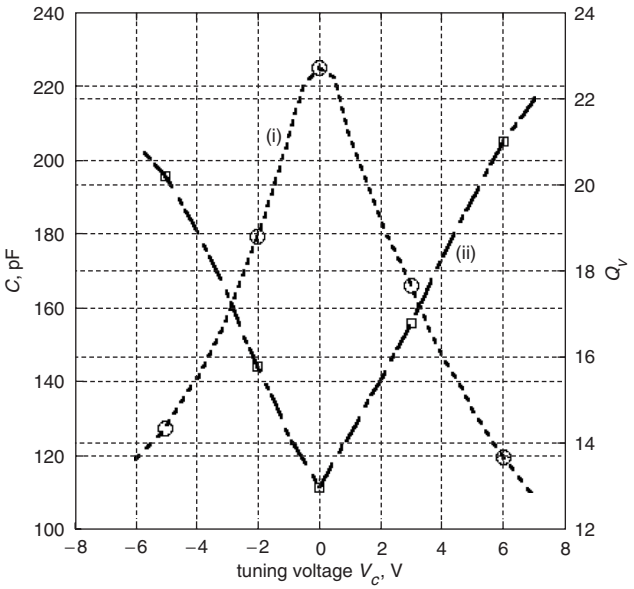

Fig. 4 *Measured BST varactor characteristics at 50 MHz*
(i) Capacitance; (ii) Q

4.1 VCO operation

The measured frequency tuning curves of the VCOs are shown in Fig. 5. As designed, the two VCOs have almost

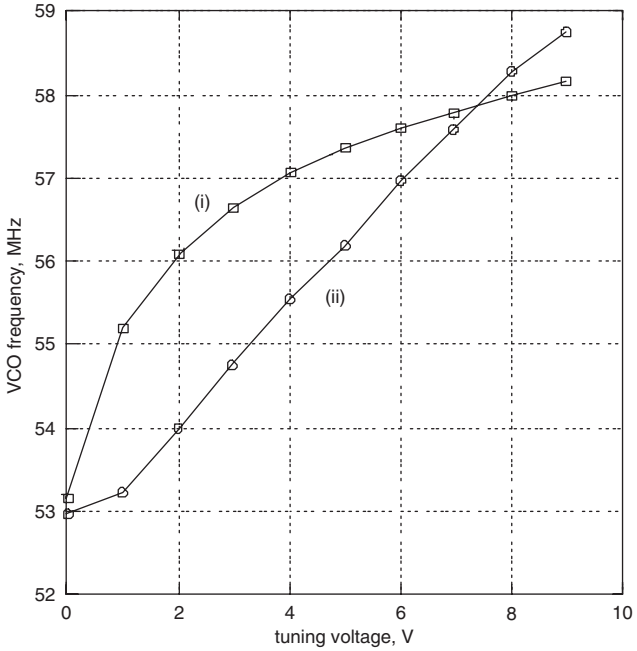

Fig. 5 *VCO frequency against tuning voltage*
(i) Junction-VCO; (ii) BST-VCO

the same tuning range. One notable difference in the tuning characteristics is the nearly linear tuning curve of the BST-based VCO. Apart from tuning range, the most important characteristic of a VCO is phase noise. Oscillator phase noise is a single-sided power spectral density of phase fluctuation and for this work measurements were performed using an Agilent Model 4352B Signal Analyzer test set. During noise measurements the circuits were operated on battery and shielded to eliminate extraneous sources of noise. Single-sided phase noise measurements were taken at offset frequencies of 100 Hz–1 MHz, while spot noise measurements were taken at 1 and 10 kHz. The single-sided noise power spectra of the junction-varactor VCO operating in normal mode (mid-tuning range), at 0 V bias, and near reverse breakdown are shown in Fig. 6. The BST varactor VCO single-sided phase noise is shown in Fig. 7 under similar conditions. The phase noise responses of the two VCOs have different characteristics which can be interpreted in terms of Q variation, nonlinear effects and excess shot noise. In this Section we will focus on the overall noise characteristics and in the next Section we will address the phase noise slope characteristics.

In Fig. 6 the phase noise of the junction VCO is seen to be a strong function of tuning voltage. Curve (iii) in Fig. 6 corresponds to operating near reverse breakdown, where excess phase noise results, leading to significantly higher phase noise than when the varactor is biased away from breakdown. At 0 V bias, curve (ii) in Fig. 6, the excess phase noise that comes with forward conduction is seen to increase phase noise. In contrast, excess phase noise at 0 V bias is not seen with the BST-based VCO, see curve (i) in Fig. 7, since there is no forward conduction.

It was observed that phase noise degradation occurred at a tuning voltage of 1 V and below for the semiconductor varactor-based VCO. This is attributed to the RF voltage across the varactor adding to the DC tuning voltage and resulting in conduction during part of the cycle. This is a condition likely to occur with MOPAs. Note that the topology was chosen in part because a much larger voltage swing of 90 V peak-to-peak is developed across the resonator, see Fig. 8, than across the varactors, see Figs. 9 and 10, to minimise nonlinear effects.

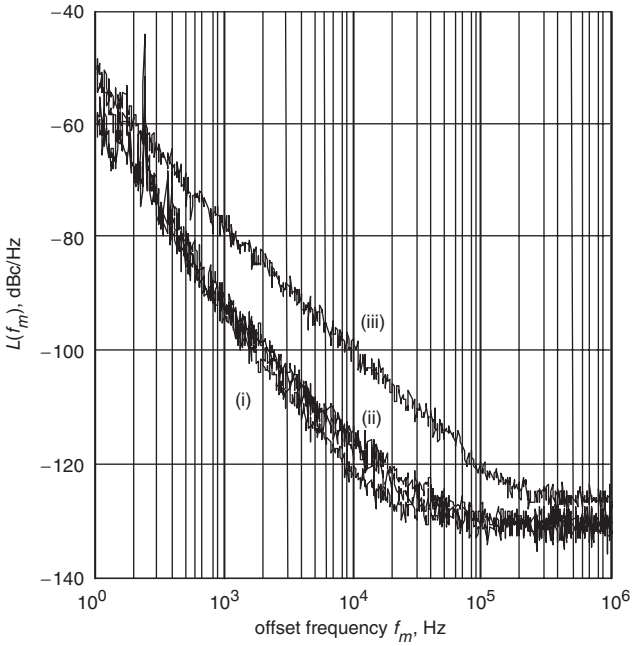

Fig. 6 *Measured single-sided phase noise of the VCO with the junction varactor against tuning voltage*
(i) 6 V; (ii) 0 V; (iii) 18 V

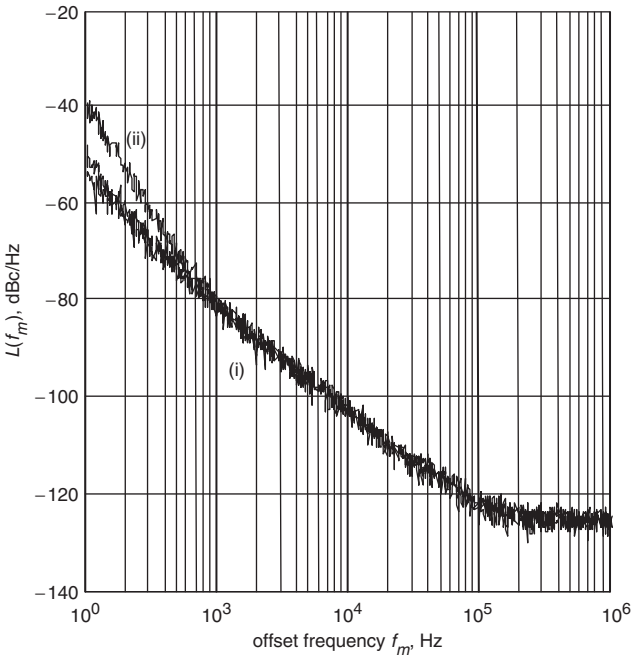

Fig. 7 *Single-sided phase noise BST varactor against voltage tuning*
(i) 0 V and 3 V overlap; (ii) 6 V

The oscillator phase noise in the tuning voltage region $V_0 < V_T < V_B$ is partially dependent on resonator Q and should match the varactor loss trends in Figs. 4 and 11. In this region, Leeson [9] predicts an oscillator phase noise $L(f_m)$ proportional to $(\omega_o/2Q)^2$. For the BST-based VCO, the correlation of the oscillator noise with Q is very good for tuning voltages between 1–6 V. In particular, the agreement based on Q ratio alone is better than 2 dB over this range, see Fig. 12. Significant departure occurs above 6 V as BST breakdown is approached. Above 6 V tuning voltage, the phase noise increases rapidly as the BST breakdown voltage

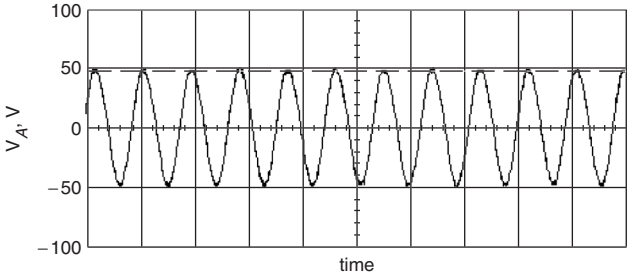

Fig. 8 *RF voltage across the resonator measured at point (A) in Fig. 3*
Time scale: 100 ns/div

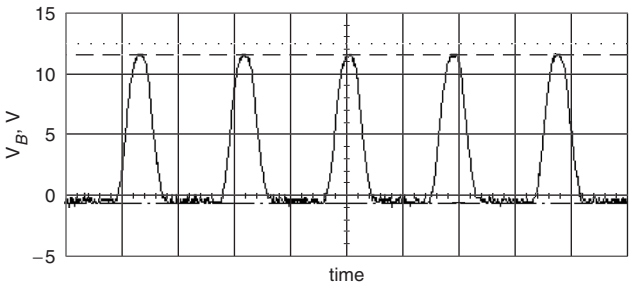

Fig. 9 *Total voltage across the junction varactor measured at point (B) in Fig. 3*
Time scale: 50 ns/div

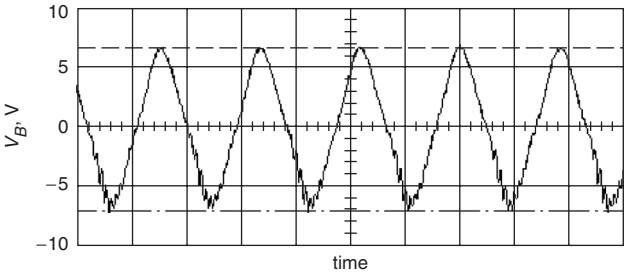

Fig. 10 *Total voltage across the BST varactor measured at point (B) in Fig. 3 (tune voltage = 0 V)*
Time scale: 50 ns/div

is approached, curve (ii) in Fig. 12. Rapidly increased phase noise is seen in Fig. 13 for the junction varactor-based VCO. In addition forward-bias conduction in the junction varactor also contributes to phase noise degradation. This can be seen by contrasting curves (i) and (ii) in Fig. 6. The phase noise at 6 V bias, curve (i), corresponds to the no-conduction condition, but curve (ii), the phase noise at 0 V bias, has excess noise resulting from shot noise. The corresponding results for the BST varactor, the superimposed curves (i) in Fig. 7 show no difference between the zero-bias condition and moderately-biased (3 V) conditions.

The above discussions are supported by the measured resonator and varactor voltages reported in Figs. 8–10 and obtained using high impedance probes. The resonator voltages for both the BST and junction varactor-based VCOs were 90 V peak-to-peak and are shown in Fig. 8. The voltages are identical as circuit conditions were adjusted to achieve this. The voltage across the junction varactor is shown in Fig. 9, where it is clear that the varactor voltage is limited by forward conduction to 0.7 V. There is clearly significant harmonic content. The voltage across the BST varactor (at 0 V bias) is shown in Fig. 10 and there is little harmonic content. Spectrum analysis of the VCO output

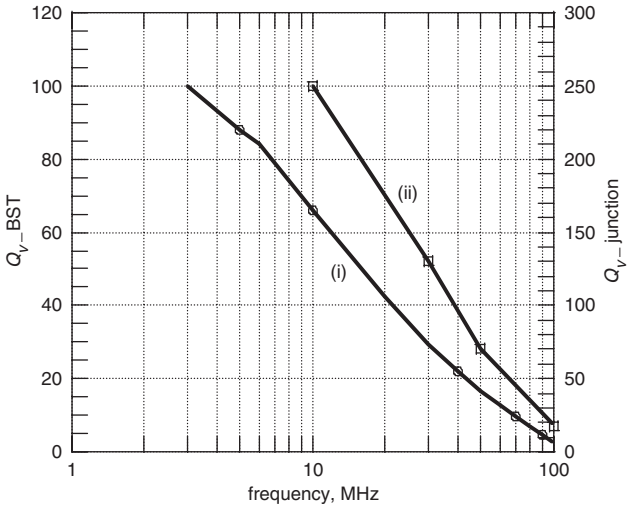

Fig. 11 *Calculated Q as a function of frequency*
(i) BST varactor; (ii) junction varactor
Tune voltage is 4 V

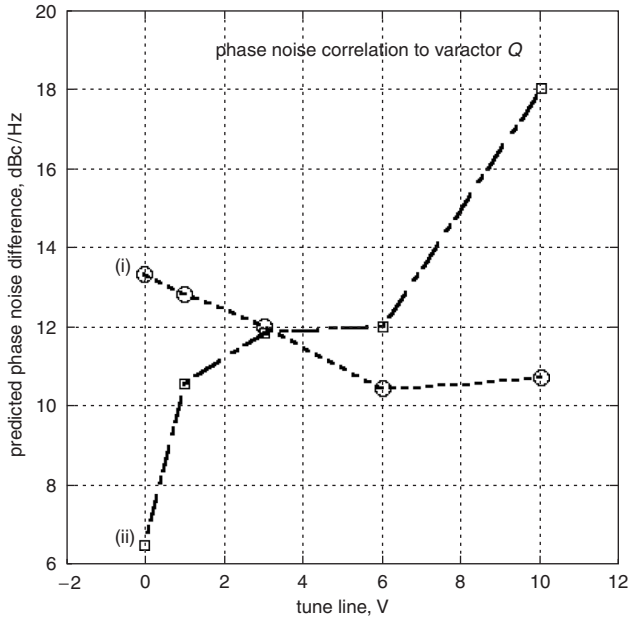

Fig. 12 *Relative phase noise against tuning voltage for the BST-based VCO*
(i) Predicted from Leeson's model; (ii) measured

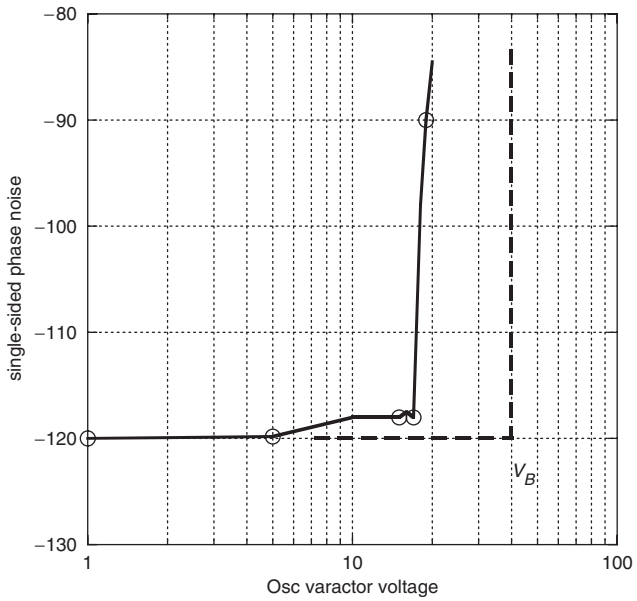

Fig. 13 *Measured junction varactor phase noise degradation against tuning voltage measured at point (C) in Fig. 3*
Breakdown voltage V_B is also indicated

also showed the harmonic content of the BST-based oscillator to be much less than that with the junction varactor [8].

4.2 Phase noise slope

The phase noise plots of Figs. 6 and 7 describe the oscillator condition at 0 V, in the mid tuning range, and near breakdown. In the mid tuning range (curve (i) in Fig. 6 for the junction-varactor-based VCO and curve (i) in Fig. 7 for the BST-varactor-based VCO) there should be no excess shot noise from forward conduction or reverse breakdown. Indeed the phase noise slope with respect to frequency tracks that expected of an oscillator. The classic theory for a low Q resonator is that close to the carrier frequency, flicker noise dominates and the phase noise will have a slope of -30 dB/decade (i.e. a $1/f_m^3$ dependence). At what is known as the oscillator corner frequency, the slope changes to -20 dB/decade (i.e. there is a $1/f_m^2$ dependence). Eventually at frequencies further from the carrier the noise floor dominates. This characteristic is seen for both VCO types, see Figs. 6 and 7, and for both VCOs biased in the mid tuning region the corner frequency is approximately 1 kHz. When shot noise becomes significant the characteristic changes. First consider the junction-varactor-based VCO. At 0 V tuning the sum of the DC voltage and the RF peak voltage will lead to forward conduction at least for part of the RF cycle. This results in excess phase noise as seen in curve (ii) in Fig. 6. As reverse breakdown is approached avalanche noise dominates, see curve (iii) in Fig. 6. The slope of the phase noise above the noise floor is -20 dB/decade over the whole range and flicker noise is not evident. With the BST-varactor-based VCO the phase noise at 0 V bias is identical to that in the mid tuning range, curve (i) in Fig. 7, as there is no shot noise at maximum capacitance. However, there is an increase in shot noise at high bias when the BST varactor enters the avalanche regime during part of the RF swing. Curiously the slope of the phase noise is -40 dB/decade (i.e. a $1/f_m^4$ dependence) close into the carrier.

5 Conclusions

Two voltage-controlled oscillators (VCOs) based on junction semiconductor and BST varactors were contrasted. The development of design formulas for the oscillator tuning range enabled near optimum and closely matched VCOs to be designed leading to a fair comparison of the two technologies. This work showed that a VCO utilising a BST varactor is viable with interesting phase noise characteristics. In particular the absence of excess shot noise at maximum capacitance tuning (since there is no forward conduction) makes it a particular attractive component for a master oscillator power amplifier or MOPA.

6 Acknowledgments

The authors thank S. Lipa for his assistance in noise measurements. This work was supported in part by U.S. Army Research Office as a Multi-disciplinary University Research Initiative on Multifunctional Adaptive Radio

Radar and Sensors (MARRS) under grant number DAAD19-01-1-0496, and an NSF/ITR grant number NSF 0113350 entitled 'ITR/SI-Adaptive Integrated Radio Frequency Transceiver Front ends for High Data Rate Wireless Communications'.

7 References

1 Knights, A.P., and Kelly, M.J.: 'Laterally stacked varactor formed by ion implantation', *Electron. Lett.*, 1999, **35**, (10), pp. 846–847
2 Dongsu, K., Yoonsu, C., Allen, M.G., Kenney, J.S., and Kiesling, D.: 'A wide-band reflection-type phase shifter at S-band using BST coated substrate', *IEEE Trans. Microw. Theory Tech.*, 2002, **50**, (12), pp. 2903–2909
3 Acikel, B., Taylor, T.R., Hansen, P.J., Speck, J.S., and York, R.A.: 'A new high performance phase shifter using $BaxSr_{1-x}$ TiO_3 thin films', *IEEE Microw. Wirel. Compon. Lett.*, 2002, **12**, (7), pp. 237–239
4 Cole, M.W., and Joshi, C.: 'Fabrication and characterization of doped barium strontium titanate thin films for tunable device applications'. Proc. IEEE Antennas and Propagation Society Int. Symp., 16–21 July 2000, pp. 384–387
5 Subramanyam, G., Mohsina, N., Al Zaman, A., Miranda, F., Van Keuls, F., Romanofsky, R., and Warner, J.: 'Ferroelectric thin-film based electrically tunable Ku-band coplanar waveguide components'. 2001 IEEE MTT-S Int. Microwave Symp. Digest, 20–25 May 2001, pp. 471–474
6 Tombak, A., Maria, J.P., Ayguavives, F.T., Zhang Jin, J., Stauf, G.T., Kingon, A.I., and Mortazawi, A.: 'Voltage-controlled RF filters employing thin-film barium-strontium-titanate tunable capacitors', *IEEE Trans. Microw. Theory Tech.*, 2003, **51**, (2), pp. 462–467
7 ATMI, Inc. Danbury, CT. http://www.atmi.com
8 Victor, A., Nath, J., Ghosh, D., Boyette, B., Maria, J.-P., Steer, M.B., Kingon, A.I., and Stauf, G.T.: 'A voltage controlled oscillator using barium strontium titanite (BST) thin film varactor'. Proc. IEEE Radio and Wireless Conf. (RAWCON) 2004, 19–22 Sept. 2004, pp. 91–94
9 Leeson, D.B.: 'A simple model of feedback oscillator noise spectrum', *Proc. IEEE*, 1996, **54**, (2), pp. 329–330
10 del Mar Hershenson, M., Hajimiri, A., Mohan, S.S., Boyd, S.P., and Lee, T.H.: 'Design and optimization of LC oscillators'. IEEE Int. Conf. on Computer Aided Design, 7–11 Nov. 1999, pp. 65–69
11 Underhill, M.J.: 'Fundamentals of oscillator performance', *Electron. Commun. Eng. J.*, 1992, **4**, (4), pp. 185–193
12 Underhill, M.J.: 'Reduction of phase noise in single transistor oscillators'. European Frequency and Time Forum, 1996, pp. 476–490
13 Rogers, J.M., Macedo, J.A., and Plett, C.: 'The effect of varactor nonlinearity on phase noise of completely integrated VCOs', *IEEE J. Solid-State Circuits*, 2000, **35**, (9), pp. 1360–1367

8 Appendix

The aim here is to develop a Q reduction factor Q_{0VM}/Q_0 in terms of the varactor capacitance tuning range $\hat{\alpha}$ (12) the normalised frequency tuning variable $\hat{\chi}$ (13) and the q factor (18). The development begins by expanding (13) in terms of the resistance ratio R/R_S and noting that $R/R_S = Q_0 Q_V C_V/C$. In the same step we use the relation that the Q of the tank circuit is $Q_0 = \omega_{0V} RC$ at the resonant frequency, ω_{0V} of the varactor-loaded tank circuit. This results in

$$Q_{0V} = \frac{Q_0}{1 + \dfrac{Q_0 C_V}{Q_V C}} + \frac{Q_0 (Q_V/Q_0)}{1 + \dfrac{Q_V C}{Q_0 C_V}} \tag{20}$$

The minimum value of this Q_{0VM} occurs when the varactor Q is minimum, i.e. $Q_V = Q_{0VM}$, which corresponds to maximum varactor capacitance, i.e. $C_V = C_{VM}$. Thus

$$Q_{0VM} = \frac{Q_0}{1 + \dfrac{Q_0 \hat{C}_{V0}}{Q_{VM} C}} + \frac{Q_0 (Q_{VM}/Q_0)}{1 + \dfrac{Q_{VM} C}{Q_0 \hat{C}_{V0}}} \tag{21}$$

Introducing the effective varactor capacitance tuning factor $\hat{\alpha} = \hat{C}_{V0}/\hat{C}_{VB}$ results in

$$Q_{0VM} = \frac{Q_0}{1 + \dfrac{\alpha Q_0 \hat{C}_{VB}}{Q_{VM} C}} + \frac{Q_0 (Q_{VM}/Q_0)}{1 + \dfrac{Q_{VM} C}{\alpha Q_0 \hat{C}_{VB}}} \tag{22}$$

The next step is to remove specific reference to capacitance values and instead introduce the normalised tuning variable $\hat{\chi}$. Upon rearrangement and using $\hat{\alpha}$ (8) becomes

$$(\hat{\chi} + 1)^2 = \frac{C/\hat{C}_{VB} + \hat{\alpha}}{C/\hat{C}_{VB} + 1} \tag{23}$$

Rearranging again we obtain

$$\frac{C}{\hat{C}_{VB}} = \frac{\hat{\alpha} - (\hat{\chi}^2 + 2\hat{\chi} + 1)}{\hat{\chi}^2 + 2\hat{\chi}} \tag{24}$$

Now we introduce the concept of a Q loading factor $q \equiv Q_0/Q_{VM}$ as the ratio of the Q of the tank circuit to the minimum varactor Q (as measured at ω_{0V}). Consequently, we can write the Q degradation factor as

$$\rho = \frac{Q_{0VM}}{Q_0} = \left(\frac{q\hat{\alpha}(\hat{\chi}^2 + 2\hat{\chi})}{\hat{\alpha} - (\hat{\chi}^2 + 2\hat{\chi} + 1)} + 1 \right)^{-1} + \frac{1}{q} \left[\frac{\hat{\alpha} - (\hat{\chi}^2 + 2\hat{\chi} + 1)}{\hat{\alpha} q (\hat{\chi}^2 + 2\hat{\chi})} + 1 \right]^{-1} \tag{25}$$

This is the ratio of the minimum Q (Q_{0VM}) of the tank circuit with the varactor to the Q (Q_0) without the varactor for a specified normalised frequency tuning factor $\hat{\chi}$, and available capacitance tuning range $\hat{\alpha}$. The factor q is a design parameter. Q_{0VM}/Q_0 determines phase noise degradation through Leeson's formula and so ρ is an important parameter in design.